SINGLE FIBRE-TO-MORTAR BOND CHARACTERIZATION IN TRM COMPOSITES

Bahman Ghiassi[1], Ali Dalalbashi[2], Daniel V. Oliveira[2]
[1] *Department of Civil Engineering, Faculty of Engineering, University of Nottingham, Nottingham, United Kingdom, (bahman.ghiassi@nottingham.ac.uk)*
[2] *ISISE, University of Minho, Department of Civil Engineering, Guimarães, Portugal*

ABSTRACT

Textile-reinforced mortars (TRM) have been identified as sustainable materials for externally bonded reinforcement (EBR) of masonry and historical structures. The fibre-to-mortar bond, the TRM-to-masonry bond, and the mechanical properties of the TRM constituents have a fundamental role in the performance of this strengthening technique. Although several studies can be found in the literature with the focus on characterization of the tensile response and TRM-to-masonry bond behaviour, the fibre-to-mortar bond response that plays a critical role in the performance of these systems have received few attention.
This paper, as an step towards addressing the gap in characterization of the fibre-to-mortar bond behaviour, presents an experimental and analytical investigation on the effect of test setup and fiber embedded length on the pull-out response and bond-slip laws in TRM composites. Three different pull-out test setups, consisting of one pull-pull and two pull-push configurations, are developed and investigated for characterization of the single fibre-to-mortar bond behaviour. The experimental and analytical results are discussed and presented and bond-slip laws are extracted for each test setup and embedded length.

KEYWORDS

Strengthening and repair; Experimental study; Bond and interfacial stresses; FRC and cement composite materials; TRM; Pull-out test.

INTRODUCTION

Textile Reinforced Mortars (TRMs) have recently received extensive attention as a sustainable solution for externally bonded reinforcement of masonry and historical structures. TRMs provide several advantages, compared to conventional Fibre Reinforced Polymers (FRPs) including physical and mechanical compatibility with the masonry substrate, acceptable performance under high temperatures and fire exposure, and low installation costs (Ghiassi et al. 2016; Leone et al. 2017; Caggegi et al. 2017; De Stantis et al. 2017).
These composites are made of continuous fibres embedded in an inorganic (cementitious or lime-based) matrix. Cementitious mortars are usually used for application to new buildings or concrete structures and lime-based mortars are suggested for application to existing masonry and historical structures. Several types of fibres including steel, glass, basalt and PBO are available in the market as the reinforcement. The large variety of available fibres and mortar types leads to a wide range of TRMs with different mechanical and physical properties. Mechanical properties of TRMs and TRM-strengthened structural components are strongly dependent on the mortar and fibre properties, the fibre-to-mortar bond behaviour and the TRM-to-masonry bond response (Ghiassi et al. 2016). While several studies can be found in the literature devoted to characterization of mechanical properties of TRMs, e.g. (Larringa et al. 2013; Caggegi et al. 2017; Leone et al. 2017), or to the characterization of TRM-to-masonry bond behaviour, e.g. (Razavizadeh et al. 2014; Ascione et al. 2015), the fibre-to-mortar bond response in these systems has only received a limited attention (Ghiassi et al. 2016). A clear understanding of this mechanism is however critical for fully utilization of this strengthening system and, without any doubt, requires special attention (Ghiassi et al. 2016).
A variety of test methods have been developed in the literature for characterization of the fibre-to-mortar (or matrix) bond behaviour. These include the single fibre pull-out tests in which the load is applied to the fibre and can be generally categorized into pull-push or single-sided (Sahnnag et al. 1997; Sueki et al. 2007; Baena et al. 2016) and pull-pull or double-sided (Huang et al. 2016; Li et al. 2018) configurations. While in these test methods the fibre is directly loaded, in other cases the matrix is directly loaded (such as tensile tests on FRPs). Single fibre pull-out tests are generally more suitable for composites made of brittle matrices that show several transverse cracking due to the fibre bridging as is the case of TRMs (Zhandarov and Mader 2005).
It is clear that the choice of a suitable test setup should be based on producing a similar-to-reality stress distribution in the test specimens. This paper presents an experimental investigation on characterization of fibre-to-mortar

interface in TRM composites with the aim of single fibre pull-out tests. Different fibre pull-out configurations, including two pull-push and one pull-pull, are considered to evaluate the differences between obtained experimental results and their effect on the extracted bond-slip laws.

GENERAL DESCRIPTION OF EXPERIMENTAL TESTS

The materials included a unidirectional ultra-high tensile strength steel fibre (with a density of 670 g/m^2, an effective area of one cord (five filaments) equal to 0.538 mm^2 and the cord diameter of 0.827 mm) as the reinforcing material and a commercially available hydraulic lime based mortar as the matrix. The main materials mechanical properties including the compressive and flexural strength of the mortar and the tensile strength of the steel fibres were characterized following relevant standards and test procedures. The compressive and flexural tests were performed according to ASTM C109 (2005) and EN 1015-11 (1999). Cubic 50×50×50 mm^3 and prismatic 40×40×160 mm^3 specimens were prepared for compressive and flexural tests, respectively. The tests were carried out with a Lloyd testing machine under force-controlled conditions at a rate of 2.5 N/s (for the compressive tests) and 10 N/s (for the flexural tests). The results are presented in Table 1 as the average of five tested specimens. As for the steel fibres, direct tensile tests under displacement controlled conditions and with the rate of 0.3 mm/min were conducted to obtain their tensile strength and elastic modulus. The specimens had a free length of 300 mm and their deformation was measured with a 100 mm clip gauge attached to the centre of the specimens. The results showed an average tensile strength of 3141 [MPa] and elastic modulus of 174.87 [GPa].

Table 1: Mortar test methods and mechanical properties.

Material	Compressive strength	Flexural strength
Standard	ASTM C109, EN 1015-11	
Specimen	50×50×50 m^3	40×40×160 mm^3
Test speed (load controlled)	2.5 N/s	10 N/s
Mortar (age 60 days)	8.81 (13.80)	2.09 (8.3)

The pull-out tests consisted of a series of single fibre pull-out tests in three different test setups. Two pull-push and one pull-pull test setups were developed for this reason (Fig. 1). The specimens included steel fibres embedded in a hydraulic lime-based mortar with an embedded length of 150 mm. Five specimens were tested in each test setup resulting in a total of 15 pull-out tests.

In the first pull-push configuration (referred as pull-push I), the specimens consisted of single fibres embedded in mortar cylinders with 75 mm diameter and 150 mm length (equal to the fibre embedded length). The tests were performed by blocking the specimens to a rigid frame and pulling the fibres from their free end (Fig. 1a). A servo-hydraulic system with a maximum capacity of 20 kN was used for performing the tests. Aluminum tabs were glued at the fibres' free end to facilitate gripping. The resultant load was measured by the load cell integrated in the testing machine and the slip of the fibre from the mortar was measured by an LVDT mounted on the fibres. A small preload was applied to the fibres to reduce their flexibility and to facilitate attachment of the LVDT to the fibres. As it was not possible to attach the LVDT base in the vicinity of the mortar-to-fibre interface, it was mounted at the distance 20 mm from the mortar surface. The slip was then calculated as the recorded displacements minus the elastic elongation of the unbonded textile.

In the second test setup (referred as pull-push II), the specimens consisted of single fibres embedded in rectangular prism mortar with the dimensions of 150×125×16 mm^3. The free length of the fibres was embedded in an epoxy resin block over a length of 200 mm and with a rectangular cross-sectional area of 10×16 mm^2. This block, also used in Banholzer (2006), facilitates the gripping and the slip measurements in one-sided pull-out tests and protects the fibres from premature failure. Here, a U-shape steel support was used for supporting the specimens (Fig. 1a). A mechanical clamp was used to grip the epoxy resin from the top and two LVDTs were located at both sides of the epoxy block to record the slip.

In the third test setup type (pull-pull), the specimens had a geometry similar to the pull-push II test setup but they were made longer. The specimens are gripped from the bottom with a fixed mechanical gripping system in this case (and therefore the supporting system is not placed on top). Two LVDTs are again mounted on the testing block with the support placed on the mortar edge to measure the slip during the tests.

All the tests were performed under displacement control conditions with reference to the internal LVDT of the system by pulling the fibres with a velocity of 0.3 mm/min.

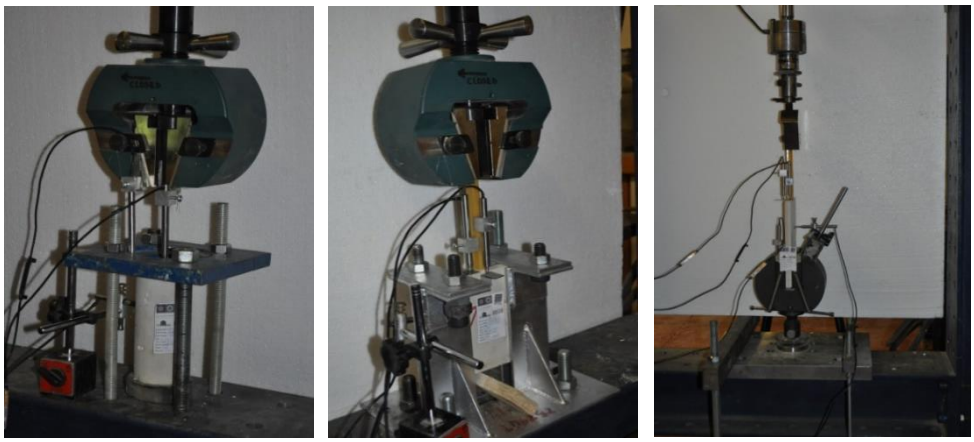

(a) (b) (c)

Fig. 1. Test setups and instrumentation used for pull-out tests: (a) pull-push I; (b) pull-push II; (c) pull-pull.

EFFECT OF TEST SETUP

The experimental envelope and average force-slip curves obtained from different test setups are shown in Fig. 2. The differences in the obtained force-slip curves is clear. It also seems that the pull-push I test setup leads to the largest variation in the results compared to the pull-push II and pull-pull tests. This was expected due to the difficulties in exact vertical alignment of the fibres in the cylindrical mortar.

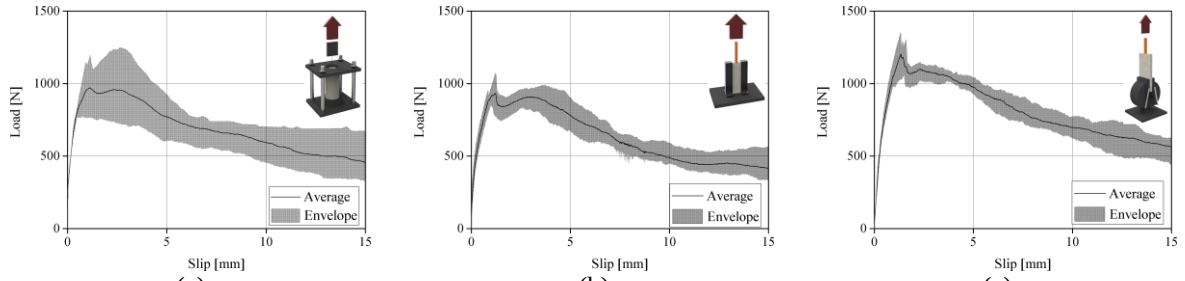

(a) (b) (c)

Fig. 2. Envelope load-slip curves for different test setups: (a) pull-push I; (b) pull-push II; (c) pull-pull.

The main outputs of single fibre pull-out tests is the force-slip curves from which the peak load, the slip corresponding to the peak load, the toughness (defined as the area of the force-slip curve until the peak load) and the initial stiffness of the pull-out curve can be extracted. These parameters are obtained from the experimental results and the average values are presented in Table 2. It can be observed that all the extracted parameters are higher in the specimens tested in pull-pull test configuration compared to the specimens tested in pull-push configuration. The reason for this is the differences in the stress distributions in the mortar, fibre and fibre-to-mortar interfaces in these two test setups. The larger initial stiffness of the specimens in pull-push II configuration, compared to pull-push I, clearly shows the effect of embedment of the free fibres in epoxy resin block on slip measurements. In pull-push I test setup, the LVDTs are mounted on the free length of the fibre (at a distance from the mortar edge) and therefore the elastic deformation of the fibre during the tests should be reduced from the measured slip values. This can lead to errors in the slip measurements and therefore increased/decreased stiffness of the elastic region in the force-slip curves. In pull-push II test setup, however, the resin block eliminates this problem. Additionally, no preloading is required in this case for attachment of the LVDTs.

The analytical formulations proposed in (Naaman et al. 1991a; Naaman et al. 1991b) were used for extraction of the bond-slip laws in the pull-pull test configuration. These formulations were modified to consider the pull-push configuration as well. For the details of the formulations and calculations the reader is referred to (Dalalbashi et al. 2018). A detailed discussion on the effect of different input parameters on the analytical bond-slip laws are also provided in this publication. Here, we only present the results obtained from the analytical modelling followed by a consistent use of input values.

It is assumed that the pull-out response consist of three main stages namely: elastic, nonlinear, and dynamic stages (Naaman et al. 1991a; Shannag et al. 1997, Mobasher 2012). The bond-slip is also defined as presented in Fig. 3. The main input values are generally the mechanical properties of fibre and mortar (including the cross section

area and elastic modulus). The analytically obtained parameters of the bond-slip law for each test setup are presented in Table 3. It can be observed that the main differences are found in the stiffness of the bond-slip curves, κ, the frictional stress, τ_f, and the slip corresponding to the initiation of the dynamic stage, S_0. The obtained bond strength is however similar ranging from 3.18 MPa to 3.2 MPa.

Table 2: Summary of the pull-out tests results (CoVs are presented in parentheses).

Specimen	Peak load [N]	Slip corresponding to peak load [mm]	Toughness until peak load [N.mm]	Initial stiffness [N/mm]
pull-push I	987 (21.8)	0.78 (40.7)	571 (56.5)	1762 (9.9)
pull-push II	992 (9.8)	1.08 (17.6)	730 (23.2)	2772 (18.2)
pull-pull	1245 (12.5)	1.33 (20.8)	1098 (30.8)	2032 (27.3)

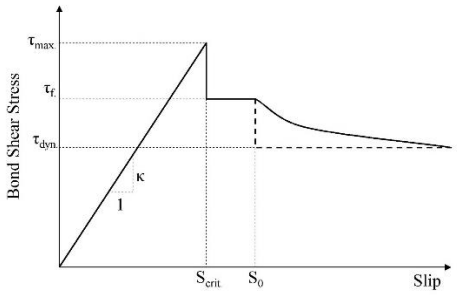

Fig. 3. Considered bond-slip law.

Table 3. Bond-slip law parameters obtained for each test setup.

Specimen	κ [N/mm^3]	τ_f [N/mm^2]	$\tau_{max.}$ [N/mm^2]	S_0* [mm]
pull-push I	9.252	2.424	3.18	0.782
pull-push II	41.777	2.499	3.27	1.045
pull-pull	5.408	3.192	3.2	0.804

*S_0 is the slip corresponding to the initiation of the dynamic stage

EFFECT OF BOND LENGTH AND MORTAR TYPE

The effect of fibre embedded length is investigated in this section. For this reason, specimens with different bonded lengths from 100 mm to 150 mm were prepared and tested with the pull-push I test setup. The results presented in the last section showed that the pull-out results in the pull-push I test setup can have similar peak forces but significantly different recorded displacements (slips) and stiffness compared to pull-push II test setup. The tests were performed on steel fibres (with properties presented before) embedded in three different mortars including two commercially available pozzolanic lime-based mortars with similar mechanical properties (denoted as A and B) and a geopolymeric-based mortar with a low mechanical properties (denoted as G) with mechanical properties shown in Table 4. Mortar A (MAPEI Planitop HDM) was a two component mortar prepared by mixing the components with an electric mixer until reaching a consistent paste as proposed in the technical datasheets. Mortar B (BASF ALBARIA STRUTTURA) was a one component mortar prepared by mixing the mortar with water (each 1 kg of mortar with 0.23 liters of water) in an electric mixer. The geopolymeric-based mortar was produced in the laboratory based on activation of alkaline materials rich in silica and alumina. The mortar was obtained by a mixture of sand (1000 gr.), fly ash (280 gr.), sodium hydroxide (144 gr.), sodium silicate (144 gr.), selected based on previous experience of the authors. Five pull-out tests were performed on each bonded length and each mortar type at the age of 60 days and the average results are presented next.

The results were obtained in terms of force-slip curves and failure mode of the specimens. The failure mode of the specimens was slipping of the fiber from the mortar in all bonded lengths and mortar types, with the exeption of SRGB specimens with l_b=200 mm in which the tensile failure of the fibers occurred. As the tensile strength of the fibers was less than the bond strength in these latter specimens, the SRGB specimens with l_b =250 mm were not tested anymore as a similar behavior (failure mode and peak load) was expected.

Table 4. Mechanical properties of mortars used for investigation of the effect of fibre embedded length (CV in round brackets).

Material	Age [days]	$f_{cm\text{-}cubic}$* [N/mm^2]	$f_{cm\text{-}cylinder}$ [N/mm^2]	E_{cm} [kN/mm^2]	f_{tm} [N/mm^2]
Mortar A	30	9.78 (9.7%)	9.85 (13.4%)	-	5.00 (13.7%)
	60	10.73 (6.7%)	10.79 (9.9%)	-	6.71 (20.8%)
	90	13.21 (10.1%)	12.74 (11.8%)	3.25 (14.6%)	6.07 (15.2%)
Mortar B	30	11.60 (13.4%)	12.66 (12.2%)	-	3.32 (5.4%)
	60	14.19 (14.3%)	-	-	3.68 (10.3%)
	90	18.12 (12.8%)	12.42 (15.4%)	14.05 (28.0%)	3.43 (11.2%)
Mortar G	30	4.16 (13.8%)	5.22 (15.7%)	-	1.68 (2.6%)
	60	3.63 (12.2%)	3.50 (21.4%)	-	1.68 (20.0%)
	90	4.19 (13.8%)	6.48 (4.0%)	13.7 (9.35%)	1.23 (16.8%)

*$f_{cm\text{-}cubic}$ is the cubic compressive strength; $f_{cm\text{-}cylinder}$ is the cylindrical compressive strength; E_{cm} is the compressive elastic modulus; and f_{tm} is the flexural tensile strength.

The average force-slip curves for different bond lengths are compared in Fig. 4. It can be observed that the maximum pull-out force (F_{max}) and the slope of the initial elastic region increase with bond length in all mortar types (until 200 mm bond length). On the other hand, no specific change in the peak slip (S_p) is observable. The peak force in SRGA and SRGG specimens increases only until bond length of 200 mm. This indicates that the effective bond length is in the range of 200 mm<le<250 mm in these systems. Razavizadeh et al. (2014) also obtained a similar numerical value for the effective bond length in a similar SRG system. On the other hand, the peak force in SRGB specimens increases until fiber tensile rupture at 200 mm bond length. The tensile rupture of the steel fiber in SRGB shows the effective bond length is in the range of 150 mm<le,<200 mm. The Fmax in SRGB specimens is always higher than SRGA which can be attributed to the higher elastic modulus of mortar B and the different bond mechanisms existing in these two systems. On the other hand, the bond strength in SRGG system is comparable to SRGA system, although mortar G has a lower mechanical properties than mortar A.

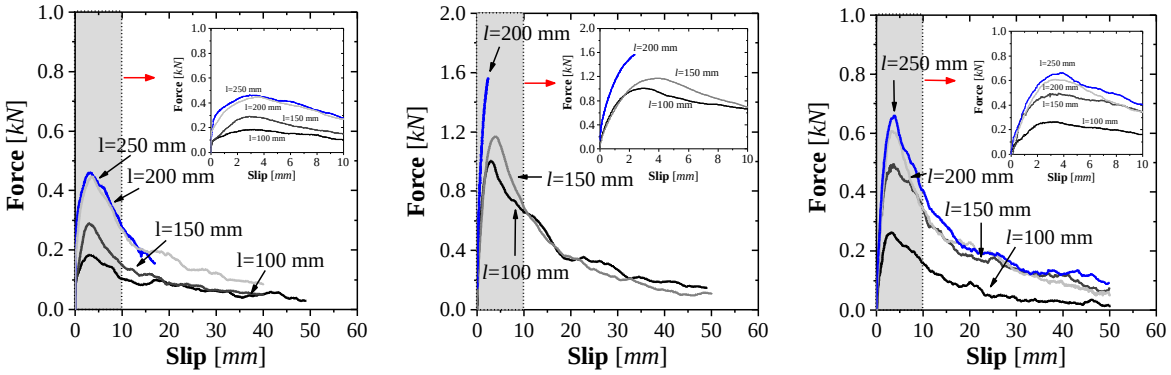

Fig. 4. Effect of fibre embedded length: (a) SRGA; (b) SRGB; (c) SRGG.

CONCLUSIONS

The effect of test setup and embedded bonded length on the fiber-to-mortar bond properties were experimentally evaluated in this study. Two pull-push and one pull-pull test setups were developed. Single fiber pull-out tests were performed on steel based TRM composites with the aim of the developed test setups. The results showed that different test setups can lead to different force-sip curves and consequently bond-slip laws. The main effect of the test setup was on the initial stiffness, frictional stress and the slip corresponding to the initiation of the dynamic stage in the extracted bond-slip laws. The bond strength was, however, found similar in all the test setup. This observation is of critical importance for interpretation and comparison of the experimental results obtained from different test setups and for proposal of reliable constitutive laws. The effect of fibre embedded length was investigated considering three different mortar type and a pull-push test configuration. The results showed the significant effect of mortar properties on the bond response. In general, the pull-push tests seem to be more suitable than pull-pull tests as the possibility of tensile cracking of the mortar at the grips is avoided. At the same time, the pull-push II tests seems to produce more reliable results and are easier to perform and are therefore suggested for further investigations.

ACKNOWLEDGMENTS

The first author acknowledges the financial support of the European Union's Marie Curie Individual Fellowship program under REA grant agreement No. 701531. This work was partly financed by FEDER funds through the Competitivity Factors Operational Programme (COMPETE) and by national funds through the Foundation for Science and Technology (FCT) within the scope of project POCI-01-0145-FEDER-007633. The support to the second author through grant SFRH/BD/131282/2017 is acknowledged.

REFERENCES

L. Ascione, G. de Felice, and S. De Santis (2015). "A Qualification Method for Externally Bonded Fibre Reinforced Cementitious Matrix (FRCM) Strengthening Systems." Composites Part B: Engineering, 78, 497-506.

ASTM C109/C109M (2005). Standard Standard Test Method for Compressive Strength of Hydraulic Cement Mortars.

M. Baena, L. Torres, A. Turon, et al. (2016). "Bond Behaviour between Recycled Aggregate Concrete and Glass Fibre Reinforced Polymer Bars." Construction and Building Materials, 106, 449–60.

B. Banholzer (2006). Bond of a strand in a cementitious matrix. Mater Struct, 39, 1015–28.

BS EN 1015-11 (1999). Methods of Test for Mortar for Masonry. Determination of Flexural and Compressive Strength of Hardened Mortar.

C. Caggegi, F.G. Carozzi, S. De Santis, et al. (2017). "Experimental Analysis on Tensile and Bond Properties of PBO and Aramid Fabric Reinforced Cementitious Matrix for Strengthening Masonry Structures." Composites Part B: Engineering, 127, 175-195.

A. Dalalbashi, B. Ghiassi, D.V. Oliveira, and A. Freitas. (2018). "Effect of Test Setup on the Fiber-to-Mortar Pull-out Response in TRM Composites: Experimental and Analytical Modeling." Composites Part B: Engineering. Under publication.

B. Ghiassi, D.V. Oliveira, V. Marques, et al. (2016). "Multi-Level Characterization of Steel Reinforced Mortars for Strengthening of Masonry Structures." Materials & Design, 110, 903–13.

L. Huang, Y. Chi, L. Xu, P. Chen, et al. (2016). "Local Bond Performance of Rebar Embedded in Steel-Polypropylene Hybrid Fiber Reinforced Concrete under Monotonic and Cyclic Loading." Construction and Building Materials, 103, 77–92.

P. Larrinaga, C. Chastre, J.T. San-Jose, et al. (2013). "Non-Linear Analytical Model of Composites Based on Basalt Textile Reinforced Mortar under Uniaxial Tension." Composites Part B: Engineering, 55, 518–27.

M. Leone, M.A. Aiello, A. Balsamo, F.G. Carozzi, et al. (2017). "Glass Fabric Reinforced Cementitious Matrix: Tensile Properties and Bond Performance on Masonry Substrate." Composites Part B: Engineering, 127, 196-214.

X. Li, J. Bielak, J. Hegger, et al. (2018). "An Incremental Inverse Analysis Procedure for Identification of Bond-Slip Laws in Composites Applied to Textile Reinforced Concrete." Composites Part B: Engineering, 137, 111–22.

B. Mobasher (2012). *Mechanics of Fiber and Textile Reinforced Cement Composites*. London- New York: Taylor & Francis Group.

A.E. Naaman, G.G. Namur, J.M. Alwan, et al. (1991a). "Fiber Pullout and Bond Slip. Ii: Experimental Validation." Journal of Structural Engineering, 117(9), 2791–2800.

A.E. Naaman, G.G. Namur, J.M. Alwan, et al. (1991b). "Fiber Pullout and Bond Slip. I: Analytical Study." Journal of Structural Engineering, 117 (9), 2769–90.

A. Razavizadeh, B. Ghiassi, and D.V. Oliveira. (2014). "Bond Behavior of SRG-Strengthened Masonry Units: Testing and Numerical Modeling." Construction and Building Materials, 64, 387–97.

S. De Santis, F. Ceroni, G. de Felice, et al. (2017). "Round Robin Test on Tensile and Bond Behaviour of Steel Reinforced Grout Systems." Composites Part B: Engineering, 127: 100–120.

M.J. Shannag, R. Brincker, W. Hansen. (1997). "Pullout Behavior of Steel Fibers From Cement-Based Composites." Cement and Concrete Research, 27(6), 925–36.

S. Sueki, C. Soranakom, B. Mobasher, et al. (2007). "Pullout-Slip Response of Fabrics Embedded in a Cement Paste Matrix." Journal of Materials in Civil Engineering, 19(9), 718–27.

S. Zhandarov, E. Mäder. (2005). "Characterization of Fiber/matrix Interface Strength: Applicability of Different Tests, Approaches and Parameters." Composites Science and Technology, 65(1), 149–60.